

Short Communication

Electrochemical and Mechanical Properties of Asphalt Concrete Modified by Carbon Microfibers

Lijie Ma^{1,2,*}, Chunfeng Yang¹, Jishu Sun¹

¹ School of Civil and transportation Engineering, Hebei University of Technology, No.5340 Xiping Road, Beichen District, Tianjin, China, 300401, China

² School of Civil Engineering, North China University of Science and Technology, No.21, Bohai Avenue, Caofeidian new town, Tangshan City, Hebei Province, 063210, China

*E-mail: Lijiema62@163.com

Received: 21 October 2019 / Accepted: 26 November 2019 / Published: 10 March 2020

Carbon microfibers (CMFs) due to their flexibility, durability, conductivity and superior strength have great potential as reinforcement materials in asphalt concrete. This work focuses on the electrochemical and mechanical properties of the CMFs modified asphalt concrete mixture. Morphological and structural analysis of the CMFs were done by scanning electron microscope, Raman spectroscopy and X-ray diffraction. Electrochemical impedance spectroscopy (EIS) technique was used for electrochemical study of asphalt concrete in deicer solutions. The EIS results revealed that a small amount of the CMFs in asphalt concrete mixtures improved remarkably corrosion resistance and increased durability of asphalt pavement. The highest amount of dynamic stability was observed in asphalt concrete with 1.0 wt% CMFs which was about 42% greater than that of without the CMFs. These results indicate that the CMFs were more effective in enhancing the dynamic stability and deformation rate, and reducing the porosity of asphalt concrete. Furthermore, the asphalt uniformity and compaction were improved by the CMFs.

Keywords: Asphalt concrete; Carbon microfibers; Electrochemical impedance spectroscopy; dynamic stability

1. INTRODUCTION

Recently, asphalt technology is an important challenge in the pavements of roads and highways which can be useful for transportation facilities. Many studies have been performed to the improvement of physical and mechanical properties of asphalts [1, 2], such as dynamic modulus [3], moisture susceptibility [4, 5] and resilient modulus [6].

Deicers are mostly used in cold weather for controlling ice and snow and maintaining high quality of winter roadways, which results in productivity, mobility and safety benefits. However, the increasing

use of deicers has raised concerns due to their effects on motor vehicles, bridge decks, pavements, and the environment. The harmful effects of deicers on asphalt concrete and their corrosion damage to the transportation infrastructure are recognized [7, 8].

Several studies have confirmed that damage of the asphalt concrete mixture with deicers is more than water. Some researchers reported that the destructive effects were observed, especially when the pavement was subjected to freeze–thaw cycles [9].

Nano- and micro-reinforced materials have the potential to use traditional materials as expandable materials. Amiri et al. had investigated that the use of carbon nanotubes in modified asphalt concrete mixtures can enhance rutting resistance [10]. Nanoclays materials modify some properties of asphalt binders, for example rutting, however, it cannot provide appropriate effect on the fatigue [11]. Carbon nanofiber has high aspect ratio, tensile strength and high modulus. Therefore, the use of these materials had resulted in significant enhancement in the mechanical and physical properties of polymer mixtures [12].

In this work, the use of carbon microfibers to modify mechanical and electrochemical properties of asphalt concrete mixtures were evaluated.

2. MATERIALS AND METHOD

In order to prepare carbon microfibers (CMFs), polyacrylonitrile and polymethyl methacrylate with a 50/50 weight ratio were dissolved in dimethylformamide to make a polymer solution (10 wt%). The solution was continuously stirred for 12 hours at room temperature. Synthesis of nanofibers was done by electrospinning technique with a high-voltage power supply (You-Shang Technical Corporation). First, the polymer solution was transferred to a 10 mL glass syringe. A high voltage (20 kV) was applied to the electrospinning needle. Aluminum foil was vertically placed at a 15 cm horizontal distance from the needle tip. A flow rate of 0.8 mL/h was fixed for the polymer solution at room temperature. After electrospinning, as-prepared CMFs were transferred to a tubular quartz furnace and treated at 800 °C for 2 hours in nitrogen flow.

Performance graded asphalt binder (PG 46-34) was applied in this study. The aggregates was included of 43% granites coarse aggregate, 45% granite crushed fines, and 15% silica sand as concrete aggregate. The CMFs was added in the composition of asphalt with different weight of 0, 0.5 and 1 wt%. The aggregates were dried at a temperature of 100 °C by a desiccator. Then, the aggregates were mixed with bitumen. During the mixing, the viscosity was kept 180 ± 20 centistoke. A compaction machine was used to construct compact asphalt concrete (compacted 70 times). Then, asphalt mortar was placed in an oven at a high curing temperature of 130 °C.

AISI 304 stainless steel with diameter of 6mm was utilized as a working electrode in EIS measurement. All steel electrodes were mechanically polished by silicon carbide sheets. Then, the stainless steels were washed with DI water under ultra-sonication. Before coating, asphalt binder was heated up to 180 °C for 20 min. Then, the CMFs were consecutively added and stirred to obtain good uniformity during heating. A few drops of asphalt binder with CMFs were poured onto the steel surface. Then, the steel was moved to the oven at the 130 °C for 10 min. The asphalt coating-steel was transferred

in laboratory environment and allowed to cool down. Afterwards, the specimens were frozen to avoid any issue of the asphalt softening. MgCl₂ Deicing chemicals was used in this study. The deicer was diluted with tap water at ratio of 1:5 (deicer:water) which was used as an electrolyte solution in EIS tests.

EIS (CorrTest Instruments Corp., Ltd., China) tests were conducted at open circuit potential with a scanning range of 10 mHz to 100 kHz at the amplitude of 10 mV. ZSimpWin was used to interpret the experimental results. The morphologies of the samples corroded in the deicer solution for 5 h were examined using scanning electron microscope (SEM, FEI/Nova NanoSEM 450). Structure analysis of CMFs was performed with X-ray diffraction (Xpert Pro, Philips. Company) with the CuK α radiation 1.5404 Å wavelength at 40 KV/30 mA. Raman spectroscopy was done by a LabRAM-HR800 Raman microscope with the wavelength of incident laser light.

A square plate mold with a 300 mm width and a 50 mm height was used to make wheel tracking test samples for dynamic stability. After pouring the asphalt mortar into the silicone mold, a roller compacter was used to compact the samples.

3. RESULTS AND DISCUSSION

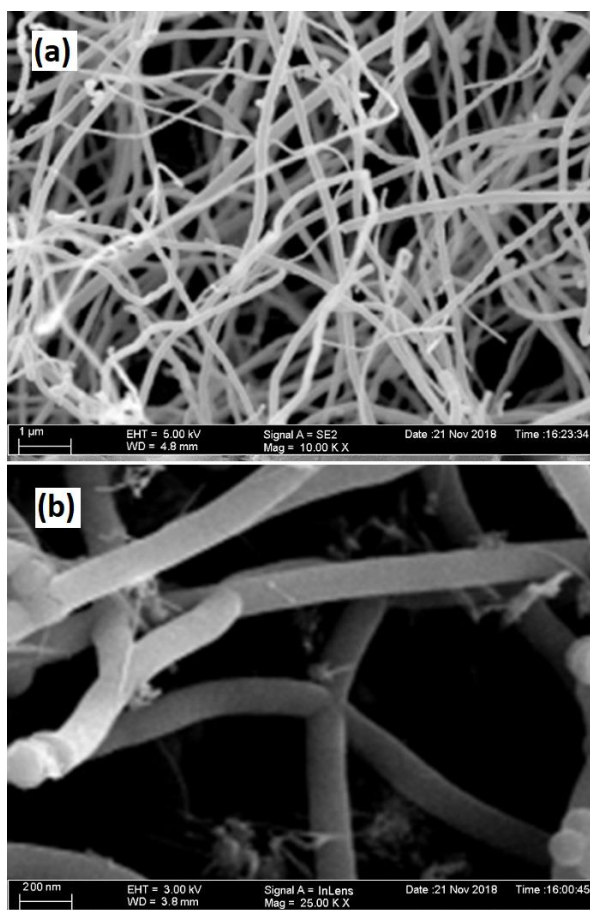


Figure 1. SEM images of the prepared carbon microfiber by electrospun technique at different magnifications (a) 10 k (b) 25 k

Figure 1 shows the FESEM images of carbon microfibers (CMF) prepared by electrospinning technique in a wide diameter range from 100 nm to 200 nm. Although the length measurement of CMFs was really difficult, the ratio of length to diameter was estimated that can be larger than 150. Furthermore, as shown in figure 1b, the CMFs were straight, and their surface was very smooth.

Raman spectroscopy as an analytical technique was used to study the frequency and vibrational modes in the CMFs. The Raman spectrum reveals two sharp and strong peaks at 1352 and 1584 cm^{-1} , which were related to the disorder-induced D band and G band due to the high frequency first-order E_{2g} mode [13], respectively (Fig 2a). The intensity ratio of the D and G bands aids to evaluate the defects of graphene based samples. In this work the estimated intensity ratio was 0.70, which was in accordance with the commercial hollow CMF samples [14, 15]. This result indicates the good formation of CMFs.

In order to do the structural analysis of CMFs, the microfibers were characterized by nondestructive XRD technique. Figure 2b indicates the XRD analysis of the CMFs. The patterns demonstrate a strong and sharp reflection at approximately 24.5° and a weak peak near 46°, which are related to the (002) and (100) lattice planes in crystal structure of the graphite, respectively [16].

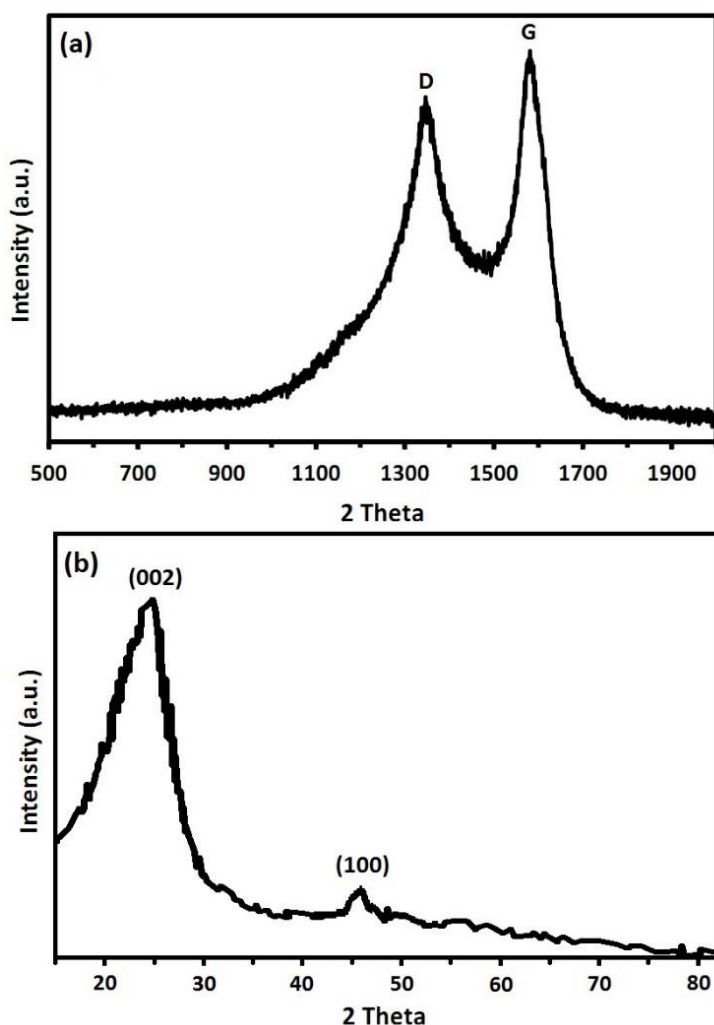


Figure 2. (a) Raman spectra and (b) XRD pattern of prepared carbon nanofibers.

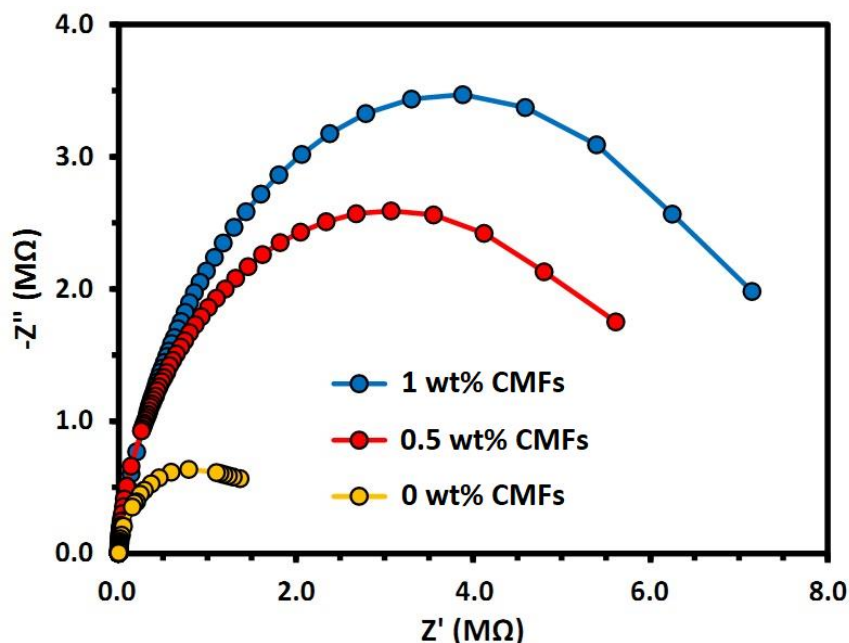


Figure 3. Nyquist diagrams attained for the asphalt mixture coated on steel in deicer solutions

Figure 3 shows the Nyquist diagrams for mixes 0, 0.5 and 1 wt% CMFs in asphalt concrete. Figure 4 indicates an equivalent electric circuit is utilized to fit EIS plots in Fig. 3. Five elements used in this circuit are included: R_s is the electrolyte resistance. C_1 and R_1 are the capacitance and resistance of asphalt mixture coated on steel, respectively; C_2 and R_2 are the double-layer capacitance and the charge transfer resistance of the steel-electrolyte interface [17]. R_s had insignificant effect on the system impedance. C_2 and R_2 describe the corrosion resistance of the steel/electrolyte interface that were not correlated with the asphalt mixture coating. Thus, in this study, the parameters of R_2 , C_2 and R_s were not considered for further analysis.

R_1 can explain the electrochemical properties of modified asphalt concrete and the solution resistance with the interconnected pores, air voids and cracks. Moreover, the thickness of the asphalt coating as a main factor to evaluate the R_1 value should be considered. To avoid this problem, the asphalt mixture thickness on all the steel specimens were controlled by the PosiTest DFT. The asphalt mixture thickness for all samples was approximately 90 mm.

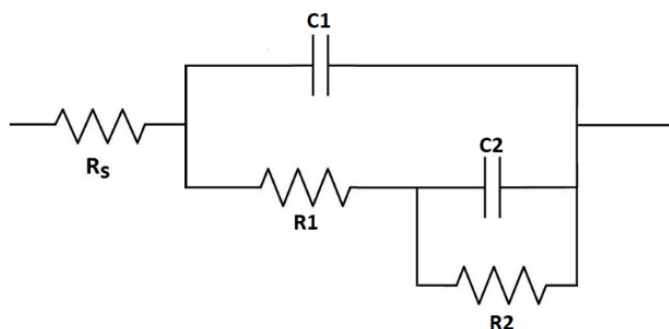


Figure 4. The equivalent circuit

The EIS plot shape for all samples indicates a common response of asphalt mixture coating immersed in electrolyte solutions. The calculated C_1 and R_1 values are summarized in table 1.

Table 1. R_1 and C_1 values of the specimens

Concentration of CMFs	R_1 ($M\Omega.cm^2$)	C_1 ($nFcm^{-2}$)
0.0 wt%	0.86	1.51
0.5 wt%	5.91	0.38
1.0 wt%	7.69	0.27

As shown, the R_1 for asphalt mixtures with 0.5 and 1 wt% CMFs was remarkably increased by 7 and 9 times than that of 0 wt% CMFs, while the C_1 was reduced by 4 and 6 times respectively. The reduction of capacitance values with increasing CMFs concentration revealed that the deicer had little influence into the asphalt mixture coating via the interconnected pores, air voids and/or cracks. The higher resistance indicates that a more uniform and compact asphalt layer was formed on the surface of steel. Furthermore, the increase of resistance with addition of CMFs can be attributed to the excellent dispersion property of the CMFs in the modified asphalt concrete. The large active surface area and high aspect ratio of CMFs resulted in the decreased size and number of pathways and pores from which the deicer can penetrate the asphalt coating. The EIS results proposed that the asphalt mixture incorporated with a small amount of microfibers can obviously enhance its ability to deal with deicer.

Figure 5 indicates the dynamic stability and deformation rate for all samples. The value of dynamic stability for asphalt concretes was significantly enhanced by incorporating CMFs. The highest amount of dynamic stability was observed in asphalt concrete with 1.0 wt% CMFs which was about 42% greater than that of without the CMFs. The deformation rate was greatly decreased by addition of CMFs, as shown in Figure 4. This means that the incorporation of CMFs in the asphalt mixture is very effective in delaying the deformation increase through wheel loads. It can be attributed to the fact that the CMFs resisted the widening and propagation of cracks created in the asphalt concrete through the wheel load.

The lowest deformation rate was also attained for the 1.0 wt% CMF sample, which was approximately 30% lower than that of CMFs free asphalt concrete. This result is significantly comparable with previous reported in modifying asphalt concrete by addition of the carbon nanotubes [18, 19] and graphite nanofibers [20].

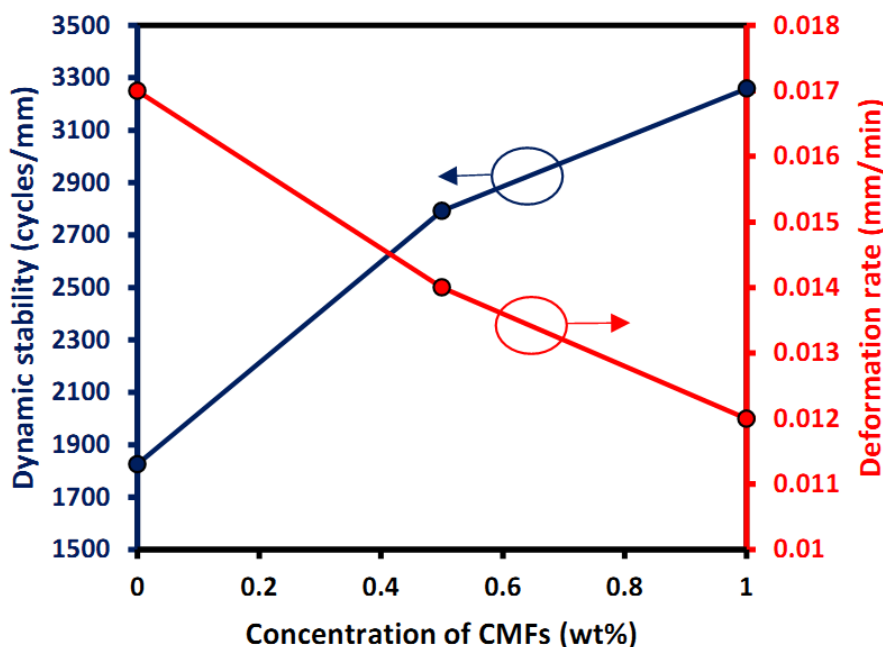


Figure 5. Effect of CMFs on deformation rate and dynamic stability of asphalt concrete

4. CONCLUSIONS

The electrochemical and mechanical properties of CMFs modified asphalt concrete mixtures were investigated. The ratio of length to diameter for produced CMFs was estimated by SEM results that can be larger than 150. The EIS results proposed that the asphalt mixture incorporated by a small amount of microfibers can obviously enhance its ability to deal with deicer solution. The higher resistance of asphalt mixture indicates that a more uniform and compact asphalt layer was formed on the surface of steel. The highest amount of dynamic stability was observed in asphalt concrete with 1.0 wt% CMFs which was about 42% greater than that of without the CMFs. The deformation rate was greatly decreased by addition of CMFs. The findings indicate the important role of microfibres to enhance the microstructural and physical properties of asphalt concrete even under corrosive solution attack.

AKNOWLEDGEMENT

This research was sponsored by Tangshan Science and Technology Project (14130247B) and Design and Application of High Modulus Asphalt Pavement Materials.

References

1. M. Gong, J. Yang, J. Zhang, H. Zhu and T. Tong, *Construction and Building Materials*, 105 (2016) 35.
2. M. Husairi, J. Rouhi, K. Alvin, Z. Atikah, M. Rusop and S. Abdullah, *Semiconductor Science and Technology*, 29 (2014) 075015.

3. P. Shao, L. Ding, J. Luo, Y. Luo, D. You, Q. Zhang and X. Luo, *ACS applied materials & interfaces*, 11 (2019) 29736.
4. S. Xu, F. Xiao, S. Amirkhanian and D. Singh, *Construction and Building Materials*, 142 (2017) 148.
5. S Kakooei, HM Akil, A Dolati, J Rouhi, *Construction and Building Materials*, 35 (2012) 564.
6. C. Li, S. Hu, L. Yang, J. Fan, Z. Yao, Y. Zhang, G. Shao and J. Hu, *Chemistry–An Asian Journal*, 10 (2015) 2733.
7. X. Shi, M. Akin, T. Pan, L. Fay, Y. Liu and Z. Yang, *Open Civil Engineering Journal*, 3 (2009) 16.
8. L. Yang, G. Yi, Y. Hou, H. Cheng, X. Luo, S.G. Pavlostathis, S. Luo and A. Wang, *Biosensors and Bioelectronics*, 141 (2019) 111444.
9. S. Luo and X. Yang, *Construction and Building Materials*, 94 (2015) 494.
10. G. Cao, L. Wang, Z. Fu, J. Hu, S. Guan, C. Zhang, L. Wang and S. Zhu, *Applied Surface Science*, 308 (2014) 38.
11. P.K. Ashish, D. Singh and S. Bohm, *Road Materials and Pavement Design*, 18 (2017) 1007.
12. P. Shao, X. Duan, J. Xu, J. Tian, W. Shi, S. Gao, M. Xu, F. Cui and S. Wang, *Journal of hazardous materials*, 322 (2017) 532.
13. E. Askari and S.M. Naghib, *International Journal of Electrochemical Science*, 13 (2018) 886.
14. S Kakooei, HM Akil, M Jamshidi, J Rouhi, *Construction and Building Materials*, 27 (2012) 73.
15. M. Saravanan, P. Sennu, M. Ganesan and S. Ambalavanan, *Journal of The Electrochemical Society*, 160 (2013) A70.
16. J. Hu, C. Zhang, B. Cui, K. Bai, S. Guan, L. Wang and S. Zhu, *Applied Surface Science*, 257 (2011) 8772.
17. B. Li, Y. Huan and W. Zhang, *International Journal of Electrochemical Science*, 12 (2017) 10402.
18. A.N. Amirkhanian, F. Xiao and S.N. Amirkhanian, *International Journal of Pavement Research and Technology*, 4 (2011) 281.
19. J. Yang and S. Tighe, *Procedia-Social and Behavioral Sciences*, 96 (2013) 1269.
20. D.-Y. Yoo, S. Kim, M.-J. Kim, D. Kim and H.-O. Shin, *Journal of Materials Research and Technology*, 8 (2019) 827.